Journal of Advanced Research 44 (2023) 201–212

Contents lists available at ScienceDirect

Journal of Advanced Research

journal homepage: www.elsevier.com/locate/jare

Original Article

CBS-H_2S axis preserves the intestinal barrier function by inhibiting COX-2 through sulfhydrating human antigen R in colitis

Shihao Guo [a,b], Zhihao Huang [a], Jing Zhu [a], Taohua Yue [a], Xin Wang [a], Yisheng Pan [a], Dingfang Bu [c], Yucun Liu [a], Pengyuan Wang [a,*], Shanwen Chen [a,*]

[a] Division of General Surgery, Peking University First Hospital, Peking University, 8, Beijing 100034, People's Republic of China
[b] Department of Colorectal Surgery, The First Affiliated Hospital of Zhengzhou University, Zhengzhou, People's Republic of China
[c] Central Laboratory, Peking University First Hospital, Peking University, 8, Beijing 100034, People's Republic of China

HIGHLIGHTS

- CBS-H_2S axis protects the intestinal barrier function.
- Hydrogen sulfide increases the sulfhydration level of HuR.
- HuR sulfhydration reduces the stability of COX-2 mRNA.
- Low expression of CBS significantly aggravated LPS-induced intestinal and systemic inflammatory symptoms.
- H_2S donor shows anti-inflammatory effects.

GRAPHICAL ABSTRACT

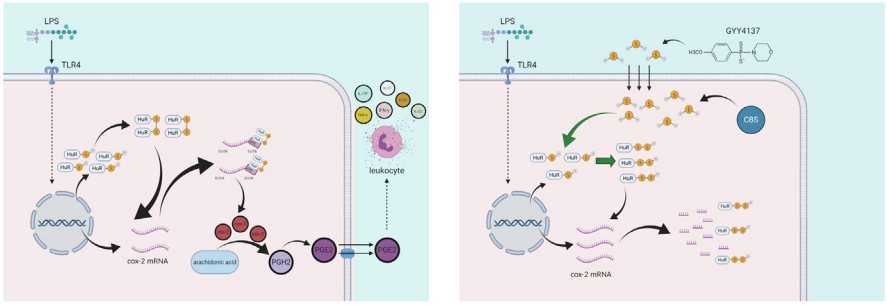

ARTICLE INFO

Article history:
Received 3 March 2021
Revised 15 July 2021
Accepted 14 March 2022
Available online 17 March 2022

Keywords:
H_2S
Colitis
Sulfhydration
COX-2
HuR

ABSTRACT

Introduction: Lipopolysaccharide (LPS) causes lesions of the epithelial barrier, which allows translocation of pathogens from the intestinal lumen to the host's circulation. Hydrogen sulfide (H_2S) regulates multiple physiological and pathological processes in colonic epithelial tissue, and CBS-H_2S axis involved in multiple gastrointestinal disorder. However, the mechanism underlying the effect of the CBS-H_2S axis on the intestinal and systemic inflammation in colitis remains to be illustrated.
Objectives: To investigate the effect of CBS-H_2S axis on the intestinal and systematic inflammation related injuries in LPS induced colitis and the underlying mechanisms.
Methods: Wild type and $CBS^{-/+}$ mice were used to evaluate the effect of endogenous and exogenous H_2S on LPS-induced colitis in vivo. Cytokine quantitative antibody array, western blot and real-time PCR were applied to detect the key cytokines in the mechanism of action. Biotin switch of S-sulfhydration, CRISPR/Cas9 mediated knockout, immunofluorescence and ActD chase assay were used in the in vitro experiment to further clarify the molecular mechanisms.
Results: H_2S significantly alleviated the symptoms of LPS-induced colitis *in vivo* and attenuated the increase of COX-2 expression. The sulfhydrated HuR increased when CBS express normally or GYY4137 was administered. While after knocking kown CBS, the expression of COX-2 in mice colon increased significantly, and the sulfhydration level of HuR decreased. The results in vitro illustrated that HuR can increase the stability of COX-2 mRNA, and the decrease of COX-2 were due to increased sulfhydration of HuR rather than the reduction of total HuR levels.

Peer review under responsibility of Cairo University.
* Corresponding authors.
E-mail addresses: pengyuan_wang@bjmu.edu.cn (P. Wang), shanwen@pku.edu.cn (S. Chen).

https://doi.org/10.1016/j.jare.2022.03.010
2090-1232/

Conclusion: These results indicated that CBS-H_2S axis played an important role in protecting intestinal barrier function in colitis. CBS-H_2S axis increases the sulfhydration level of HuR, by which reduces the binding of HuR with COX-2 mRNA and inhibited the expression of COX-2.

Introduction

The intestinal barrier plays a vital part in separating the intestinal lumen and the internal milieu, which is essential for maintaining mucosal homeostasis and immune balance [1]. During colotis, the intestinal barrier function is damaged by inflammatory cytokines, bacteria derived LPS and multiple deleterious luminal components. Meanwhile, the consequential "leaky gut" renders increased the toxic antigens entering the internal environment, which further aggravating the vicious circle composed of inflammation and intestinal barrier damage [2]. This cycle empowers the spreading of large quantities of antigens and pathogens from the intestinal lumen into the circulation, leading to systemic inflammation and distant organ injuries [3]. Thus, seeking protective reagents against intestinal barrier disfunction might provide novel therapeutic approaches for colitis.

As the third confirmed gaseous transmitter, H_2S is mainly produced by cystathionine β-synthase (CBS), 3-mercaptopyruvate sulfur transferase (3-MST) and cystathionine γ-lyase (CSE) in mammalian tissues, which is under delicate regulation in plethora of both physiological and pathological processes [4]. Cumulative studies including our previous work have validated the involvement of decreased expression of CBS-H_2S axis in multiple gastrointestinal disorders including ulcerative colitis (UC) [5]. Besides, the inhibition of the activation of NLRP-3 inflammasome and NF-kB mediated MLCK signaling have been related with the advantageous role of H_2S on the barrier function of intestine [6]. Recently, H_2S has emerged as a vital paracrine factor in the protective effect of mesenchymal stem cells in hypoxic-ischemic brain injury [7]. However, the mechanism underlying the effect of the CBS-H_2S axis on the intestinal and systemic inflammation in colitis remains to be illustrated.

As an RNA-binding protein (RBP), HuR can bind with the adenylate-rich and uranyl-rich elements (ARE) in the mRNA 3′untranslated region (3′UTR), by which increase the stability of mRNA [8,9]. The s-sulfhydration of HuR, mediated by endogenous H_2S derived from CSE, has been reported to attenuate the binding activity of HuR by breaking the disulfide bond between HuR monomer [10]. COX-2 is a critical proinflammatory enzyme in colitis, which catalyzes the conversion of arachidonic acid to prostaglandins. Recent studies have shown that the mRNA level of COX-2 is dependent on its degradation rate, which is regulated by RNA-binding proteins, including HuR [11,12]. Considering the regulatory effect of HuR on COX-2 expression, we hypothesize that the s-sulfhydration of HuR mediated by endogenous H_2S might be involved in the protective effect of CBS-H_2S axis on the inflammation localized both in the intestinal epithelium and distant organs.

In this study, LPS was used to make experimental colitis in mice. The $CBS^{-/+}$ heterozygous mice developed more severe colitis compared with WT mice, featured by the worsened clinical symptoms, increased intestinal permeability and more severe tissue injuries. The s-sulfhydration levels of HuR in $CBS^{-/+}$ mice were decreased compared with WT mice, accompanied by the augmented expression of COX-2 in $CBS^{-/+}$ mice. The regulatory effect of CBS-H_2S axis on the s-sulfhydration of HuR and the expression of COX-2 were further validated in vitro utilizing Caco-2 and HT-29 cells.

In summary, our results indicated that endogenous H_2S, mainly derived from CBS, played a vital part in keeping the integrity of the intestinal barrier function. The inhibition of HuR-COX-2 axis might be the molecular mechanism underlying the anti-inflammation function of H_2S in both intestinal epithelium and other tissues.

Materials and methods

Animals and treatment

The CBS knockdown mouse was created by Cyagen Biosciences using a CRISPR/Cas9-mediated genome-editing system; we selected exon 3 to 14 as the target sites (SI, Fig. S1A). Guide RNA and Cas9 mRNA were co-injected into fertilized eggs of C57BL/6 mouse to produce mutant lines with a 14,130 base deletion. Genotyping by PCR and DNA sequencing analysis of the founders were performed. Since all the homozygous animals with CBS knockout ($CBS^{-/-}$) died within 5 weeks of birth, so we selected the $CBS^{-/+}$ mice as the experimental animals. All $CBS^{-/+}$ mice used were obtained from heterozygous breeding with PCR analysis for the genotype detection (SI, Fig. S1B). For animal experiments with $CBS^{-/+}$ mice, littermate controls with normal CBS expression were used as WT animals. Animals were randomly allocated to experimental groups, and all $CBS^{-/+}$ mice used in this study were male mice of matched age. The mice were maintained in specific pathogen-free facilities with a standard 12 h light/dark schedule and provided standard chow and water ad libitum at the Department of Laboratory Animal Science of Peking University. Animal experiments in this study were carried out according to the Guidelines of Peking University Animal Care and Use Committee. According to the prescribed protocol, we anesthetized mice with 0.5% pentobarbital. The experimental protocol complied with the Guide for Care and Use of Laboratory Animals and was authorized by the University Ethics Committee for the use of experimental animals (201604).

The colitis model of mouse was established by injecting LPS intraperitoneally (Sigma Aldrich, America, 100 ug/10 g). 30 wt and 30 $CBS^{-/+}$ mice were stochastically grouped as follows: Control; LPS; GYY4137 + LPS. Control mice were treated with PBS 200 μL/10 g at baseline and PBS 100 μL/10 g every day from the second day. Mice in the LPS group were injected with 100 ug/10 g LPS + 100 μL/10 g PBS at baseline and 100 μL/10 g PBS every day from the second day. Mice in the GYY4137 + LPS group were injected with 500 ug/10 g GYY4137 (Sigma Aldrich, America) and 100 ug/10 g LPS at baseline and 500 ug/10 g GYY4137 every day from the second day. After 7 days of treatment, all mice were euthanized.

Clinical evaluation

We used a previous clinical score system to assess the clinical conditions of mice in each group (10 per group) [13]. The scoring method is shown in Table 1. 3 independent researchers performed the scoring work blindly.

Table 1
The scoring of clinical evaluation.

Variable	Score		
	0	1	2
Conjunctivitis	Eye closed or bleared with discharge	Eyes opened with serous discharge	Normal, no conjunctivitis
Stool consistency	Diarrhea	Loose stool	Normal stool
Hair coat	Rough and dull fur, ungroomed	Reduced grooming, rough hair coat	Well groomed, shiny fur
Activity upon moderate stimulation	Lethargic, only lifting of the head after moderate stimulation	Inactive, less alert, <2 steps after moderate stimulation	Normal locomotion and reaction, >2 steps

Paracellular permeability detection of mice intestine

Mice intestinal permeability was detected as mentioned previously [14]. On the 7th day of the animal experiment, FD-4 (150 g/L, Sigma, America) was administered to mice by gavage at a dose of 40 μL/10 g body weight. 4 h after FD-4 gavage, we collected the blood samples and detected the serum fluorescence level with Synergy H2 microplate reader (Biotek Instruments, America) with 492 nm excitation and 520 nm emission filter.

Transmission electron microscopy of colon epithelial cells

We took the first 2 cm of mouse colon (3 in each group), washed it with PBS, then fixed it with 4% glutaraldehyde, overnight at 4 °C followed by fixation with 1% osmium tetroxide. The tissue was embedded in EMbed 812 and cut into thin slices. Then the sections were stained with lead citrate and uranyl acetate, and observed with H-450 (Hitachi, Japan) transmission electron microscope.

Histological assessment of colon epithelium

The proximal colons of different groups of mice were taken and embedded with paraffin. We prepare sections and used hematoxylin and eosin (HE) to stain them. We obtained the images using Zeiss imaging optical microscopes with magnifications of 40x, 100x, and 400x. We collected at least 6 images for each slice. The extent of histopathological alterations was assessed by 3 pathologists who were unaware of grouping and grading based on a scoring method as previously mentioned [15] (Table 2).

Histological assessment of liver, lung and brain

Livers, lungs, and brains of different groups of mice were taken and embedded with paraffin. We prepared sections and used hematoxylin and eosin (HE) to stain them. We obtained the images using Zeiss imaging optical microscopes with magnifications of 200x. We collected at least 6 images for each slice and the extent of histopathological changes were scored by 3 pathologists in a "blinded fashion" to confirm the level of inflammation.

Table 2
The scoring of histological assessment.

Grade	Histological characteristic(s)
0	Normal mucosal villi
1	Subepithelial Gruenhagen's space (edema), usually at the apex of the villus
2	Extension of the subepithelial space with moderate lifting of epithelial layer from the lamina propria
3	Massive epithelial lifting down the sides of villi; a few tips may be denuded
4	Denuded villi with lamina propria and dilated capillaries exposed
5	Digestion and disintegration of lamina propria; hemorrhage and ulceration

The histopathological changes of livers were assessed by an injury grading score as previously described with modifications [16]. The scoring system was as follows: 0 = no infiltration, 1 = minimal/slight infiltration, 2 = moderate infiltration, 3 = severe infiltration and 4 = maximal infiltration.

The histopathological changes of lungs were evaluated based on Mikawa methods for lung injury pathology score: (1) alveolar congestion, (2) leukocytes infiltration, (3) hemorrhage, (4) thickness of the alveoli wall and formation of a hyaline membrane. Each item was scored on as follows: 0 = minimal damage, 1 = mild damage, 2 = moderate damage, 3 = severe damage, and 4 = maximal damage [17]. The average score of 4 indexes was calculated to evaluate the degree of lung injury.

The histopathological changes of brains were scored in line with a scoring method as mentioned previously with modifications: lesions were scored according to their severity, and the severity of each sample was overall scored using the following criteria: 0 = normal; 1 = mild; 2 = moderate; 3 = severe; and 4 = maximal severe [18].

Measurement of inflammatory cytokines in plasma

The concentrations of 18 kinds of Th1, Th2, and Th17 Cytokines in the mice plasma from each group (3 mice/group) were determined using the Quantibody® Mouse Th17 Array 1 Kit (Raybiotech, America) according to the product instructions.

Cell culture

We acquired the human colonic cell lines HT-29 and Caco-2 from the American Type Culture Collection. Caco-2 was cultured in DMEM High Glucose (BI, ISR) and HT-29 was cultured in McCoy's 5A Medium (BI, ISR), supplemented with fetal bovine serum (10% v/v), penicillin (50 U/ml), streptomycin (50 U/ml), 1% non-essential amino acids and 25 mM HEPES. Incubation was in an environment of 37℃ and 5% CO_2.

For the in vitro experiments, 10 ug/L LPS was added into the medium for 48 h to induce the cell damage with or without GYY4137 (50 μM).

Real-time quantitative polymerase chain reaction (RT-qPCR)

We utilized TRIzol onestep method (Trizol reagent; Invitrogen, America) to extract the total RNA of cells and RevertAid First Strand cDNA Synthesis Kit (Thermo Fisher, America) to reverse transcribe RNA into cDNA. PowerUp SYBR Green Master Mix (Thermo Fisher, America) was used to conduct RT-qPCR. Primers (5′-3′) were shown below: GAPDH: F, GCACCGTCAAGGCTGAGAAC; R, ATGGTGGTGAAGACGCCAGT; COX-2: F, CCCCACAGCAAACCGTAGAT; R, GGCCATGGGGTGGACTTAAA. The RT-qPCR reaction was repeated three times for each sample. GAPDH was used as internal

reference gene, and RNA relative expression was figured out by comparative threshold cycle (CT) method ($2^{-\triangle\triangle CT}$).

Western blot analysis

A method described previously was used to extract total proteins of cells [19]. We collected the mucosa of the first 2 cm colon and acquired the total protein as previously mentioned [20]. BCA method (Thermo Scientific, America) was used to detect the protein concentration, and the extracts containing same amount of proteins (20 μg) were cataphoresed in 4%-12% polyacrylamide gel. Isolated protein was transferred onto the PVDF membrane. The membrane was non-specifically bound (5% bovine serum albumin in TBS-Tween 20 buffer) for 1 h at room temperature. 0.1% rabbit anti-CBS monoclonal antibody (Invitrogen, America), 0.1% rabbit anti-COX-2 monoclonal antibody (CST, America), 0.1% rabbit anti-ELAVL1/HuR monoclonal antibody (CST, America), 0.1% rabbit anti-β-actin antibody (CST, America), and 0.1% rabbit anti-GAPDH monoclonal antibody (CST, America) were used to incubate the membrane for the night at 4℃. Then we used the secondary antibody to incubate the membrane for 1 h at room temperature, and used ECL detection reagent to perform blots (Merck Millipore, America).

Biotin switch assay of S-sulfhydration

With reference to the previously described method, a modified biotin switch assay was used to detect the level of sulfhydration [21]. In short, HEN buffer (HEPES-NaOH (pH 7.7 250 mM) with neocuproine (0.1 mM) and EDTA (1 mM)) with protease/phosphatase inhibitors, 1% Nonidet-P40 (NP-40), and 150 μM deferoxamine were utilized to homogenize the cells or tissue samples. We sonicated the homogenized samples and centrifuged them at 13,000*g* at 4 °C for 20 min. Then we added HEN buffer with 20 mM methyl thiosulfonate (MMTS) and 2.5% SDS to the lysate and shaken for 30 min at 50 °C. Next, the acetone was added to the samples to remove MMTS. Meanwhile, we precipitated the protein for 1 h at −20 °C. HEN buffer with 4 mM biotin-HPDP and 1% SDS was used to resuspend the pellets. After incubating at 25 °C for 3 h, acetone was used to purify the protein. In the end, we dissolved the protein in solution buffer and purified it with streptavidin-agarose beads, then the sulfhydrated protein was examined by Western blot. Negative controls were from cells treated by dithiothreitol (DTT) (1 mmol/L).

CRISPR/Cas9 mediated knockout of CBS in cells

The CRISPR/Cas9 system was used to achieve stable knockout of CBS in Caco-2 and HT-29 cells. In short, the interference target sgRNA was designed based on the sequence of the CBS gene as shown below: CTGATGAGATCCTGCAGCAG. We phosphorylated, annealed, and cloned the guide oligonucleotide into the BsmBI site of the pHBLV-U6-gRNA-EF1-CAS9-PURO vector (Hanbio Biotechnology, China) followed by verifying the constructed vector by sequencing. Then we transformed the transfer plasmid with guide oligonucleotide into Escherichia coli DH5α, and used Plasmid DNA purification kit (Macherey-Nagel, Germany) to isolate the plasmid from bacteria. Transferable lenti-CAS-puro plasmid (Hanbio Biotechnology, China), packaging plasmids psPAX2 (Hanbio Biotechnology, China) and pMD2G (Hanbio Biotechnology Co., Ltd., China) were transfected into 293 T cells to produce the lentivirus. 48 and 72 h after transfection, we collected the virus-containing supernatant, then transfected Caco-2 or HT-29 cells with the supernatant. Fresh medium containing puromycin (10 mg/L) was utilized for replacing the medium containing lentivirus after infected for 16 h. After 7 days of screening, we collected the puromycin-resistant cells. In the end, western blot was used to detected the cell infection efficiency.

Hydrogen sulfide determination

To detect the inhibition of cellular H_2S synthesis after CBS knockout, a fluorescent probe kindly provided by Professor Long Yi was used in line with the manufacturer's recommendations [22]. Briefly, we used a glass-bottom plate (Corning, America) to inoculated WT and $CBS^{-/+}$ cells ($\sim 2 \times 10^4$ cells/well) and cultured cells for 24 h. Then the H_2S probe (10 μmol/L) was incubated with cells for 30 min. Finally, wash cells with PBS for twice and visualize the fluorescence under Fluoview 1000 confocal microscope (Olympus, Japan).

Plasmid transfection

The plasmid pENTER-flag-6x His-HuR^{WT} and pENTER-flag-6xHis-HuR^{C13A} were purchased from Vigene Biosciences (Shandong, China). DNA sequencing was used to confirmed the successful single-site mutation of Cys13 to alanine. In line with the manufacturer's recommendations, Lipofectamine 3000 (Thermo fisher, America) was used to transfect the expression plasmids into cells. After transfected for 24 h, the cells were studied, and cells transfected with pENTER, which is the empty vector, were used as negative control.

ActD chase assay

For the ActD (Sigma, America) chase assay, we treated Caco-2 cells with ActD (10 μg/ml) alone or ActD + GYY4137 (50 μM) in serum free medium. Then we collected cells every hour for 6 h and utilized RT-qPCR to examine the expression of COX-2 mRNA. The relative mRNA expression at different time points was calculated as the fold change from the baseline.

Statistical analysis

We used the two-tailed Student's *t*-test (unpaired) and one-way ANOVA to analyze the differences in mean values between the groups (GraphPad Prism version 8.0 for Windows, GraphPad Software, America). P value < 0.05 indicates statistical significance, and all results were expressed as means ± standard error of the mean (SEM). To ensure the reproducibility, all experiments were repeated at least three times. Standard deviation was shown by error bars. * P < 0.05, ** P < 0.01, vs control group. # P < 0.05, ## P < 0.01, vs LPS group. △ P < 0.05, △△ P < 0.01, WT vs $CBS^{-/+}$ group.

Results

H_2S ameliorated clinical symptoms and preserved the intestinal barrier in experimental colitis

Decreased expression of CBS in colon epithelium of $CBS^{-/+}$ mice was validated by western blot analysis (Fig. 1A and B; SI, Fig.S2A) and IHC (SI, Fig.S1C and D). The weight and clinical score of WT mice in LPS group began to decrease significantly 1 day after LPS treatment, and decreased to the lowest level at day 3, then gradually recovered during day 4–7 compared with the control group. Weight and clinical scores of WT mice in GYY4137 + LPS group displayed no significant difference compared with those in LPS group during day 1–3, but revealed a faster recovery rate during day 4–7 compared with LPS group (Fig. 1C and G). The weight and clinical score of $CBS^{-/+}$mice in LPS group decreased continuously during day 1–4, and gradually recovered during day 5–7. The weight

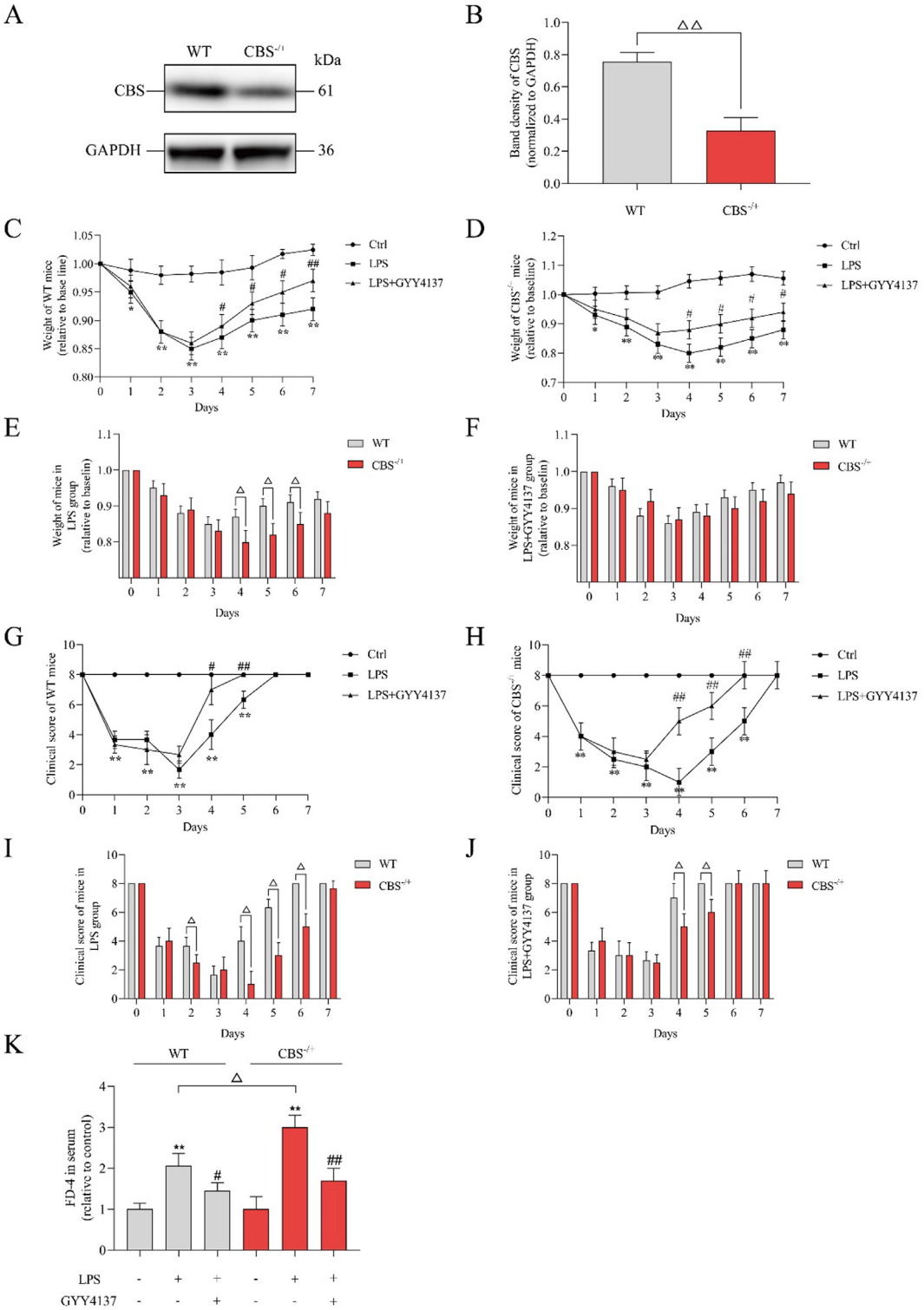

Fig. 1. CBS knockdown exaggerated the experimental colitis induced by LPS. WT and CBS$^{-/+}$ mice were intraperitoneally administered with LPS (100 ug/10 g) alone or LPS + GYY4137 (500 ug/10 g). **(A)** Representative western blot images of CBS in mice colon epithelial cells. **(B)** Relative band density of CBS in western blot. **(C)** Body weight changes of WT mice in 7 days. **(D)** Body weight changes of CBS$^{-/+}$ mice in 7 days. **(E)** Comparison of weights between WT and CBS$^{-/+}$ mice from LPS group in 7 days. **(F)** Comparison of weights between WT and CBS$^{-/+}$ mice from LPS + GYY4137 group in 7 days. **(G)** The clinical score changes of WT mice in 7 days. **(H)** The clinical score changes of CBS$^{-/+}$ mice in 7 days. **(I)** Comparison of clinical scores between WT and CBS$^{-/+}$ mice from LPS group in 7 days. **(J)** Comparison of clinical scores between WT and CBS$^{-/+}$ mice from LPS + GYY4137 group in 7 days. **(K)** FD-4 flux of intestine of WT and CBS$^{-/+}$ mice at the 7th day.

and clinical scores of CBS$^{-/+}$ mice in GYY4137 + LPS group decreased during day 1–3 and began to recover from day 4 with a higher recovery speed than those in LPS group (Fig. 2 D and H). The comparison of weights and clinical scores between WT and CBS$^{-/+}$ mice in LPS group during 7 days showed that the weights of CBS$^{-/+}$ mice were significant lower at day 4, 5 and 6, and the clinical scores of CBS$^{-/+}$ mice were significant lower at day 2, 4, 5 and 6, which indicated that CBS$^{-/+}$ mice showed more severe clin-

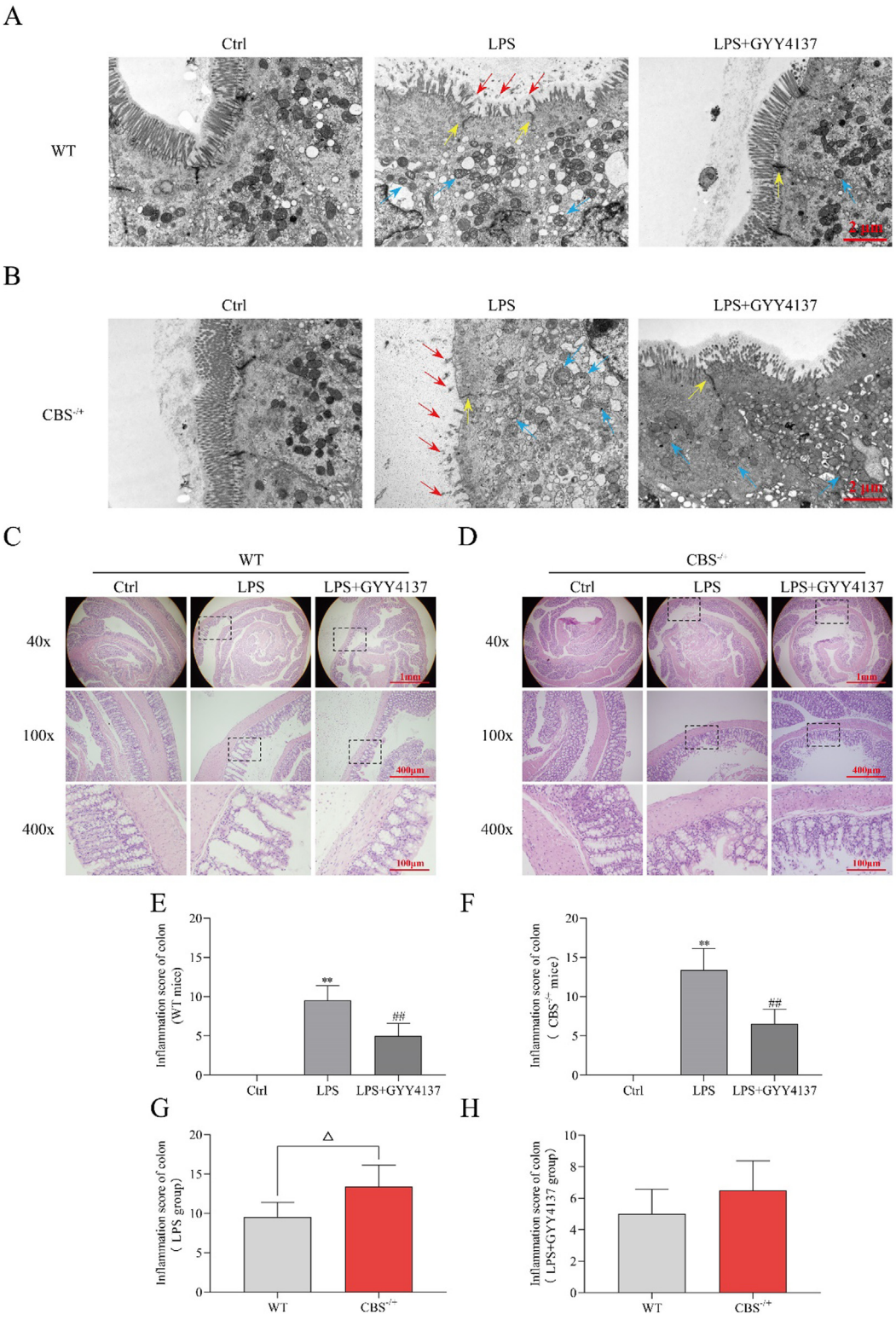

Fig. 2. CBS-H_2S axis attenuated the injuries of colon epithelium in mice with LPS-induced colitis. (A, B) Ultrastructure of colon epithelial cells of WT and CBS$^{-/+}$ mice were investigated by TEM (Red arrow: the missing intestinal villi; Yellow arrow: the incomplete TJs; Blue arrow: the swollen mitochondria). **(C, D)** Representative images of HE staining of proximal colon tissue of WT and CBS$^{-/+}$ mice 7 days after LPS administration with or without GYY4137 (40x, 100x and 400x). **(E, F)** Colon mucosal damages of WT and CBS$^{-/+}$ mice were assessed utilizing a score system. **(G)** Comparison of inflammation scores of colons between WT and CBS$^{-/+}$ mice from LPS group at the 7th day. **(H)** Comparison of inflammation scores of colons between WT and CBS$^{-/+}$ mice from LPS + GYY4137 group at the 7th day. (For interpretation of the references to colour in this figure legend, the reader is referred to the web version of this article.)

ical symptoms and lower recovery speed than WT mice after the LPS treatment (Fig. 1E and I). As for the comparison of weights and clinical scores in LPS + GYY4137 group, only the clinical scores at day 4 and 5 showed significant differences between WT and CBS$^{-/+}$ mice (Fig. 1F and J). Serum FD-4 in WT mice challenged with LPS increased by 1 time compared with control group, while FD-4

of serum from mice of LPS + GYY4137 group declined by about 25% compared with that from mice of LPS group. As for $CBS^{-/+}$mice, the increase of serum FD-4 in mice of LPS group was about 3 times, which was higher than that in WT mice. And the serum FD-4 of the $CBS^{-/+}$ mice in LPS + GYY4137 group decreased by about 50% in comparison to LPS group (Fig. 1K). The results illustrated that LPS disrupted the intestinal barrier function of mice and induced more severe colitis in $CBS^{-/+}$ mice.

H_2S improved the pathological changes in colon and distant organs in mice with colitis

To assess the injuries of intestinal epithelial tissues, TEM was adopted to investigate the status of epithelial junctions as well as subcellular changes. WT mice in control group had an intact structure of microvilli and TJs. After 7 days of LPS treatment, the missing microvilli, decreased electron-dense materials between cells, opened TJs and swollen mitochondria were observed in the colon epithelial cells. However, GYY4137 attenuated the subcellular changes of mice with colitis. As for $CBS^{-/+}$ mice, the subcellular injury was more severe in LPS group, and GYY4137 attenuated the subcellular changes (Fig. 2A and B).

The histological injuries of intestinal epithelium of each group were scored by HE staining after 7 days of LPS treatment (Fig. 2-C-H). The results indicated that the intestinal inflammatory condition of $CBS^{-/+}$ mice was exaggerated compared with WT mice after LPS treatment, and GYY4137 alleviated the histological injuries of intestinal epithelium in both WT and $CBS^{-/+}$ mice challenged with LPS. As for the distant organs, the histological scores of liver, lung and brain tissue of both WT and $CBS^{-/+}$ mice in LPS group increased at day 7 compared with the control group, while the elevated histological scores elicited by LPS was significantly attenuated by GYY4137 (Fig. 3A-D). Compared with WT mice, $CBS^{-/+}$ mice showed increased histological scores in liver and lung after 7 days of LPS treatment, while no difference shown between the two kind of mice in the LPS + GYY4137 group (Fig. 3E and F).

H_2S decreased the inflammatory cytokines level in the plasma of mice with colitis

The levels of 18 inflammatory cytokines in plasma of WT mice were examined by Quantibody® array kits. IFN-γ, IL-17F, IL-17, IL-6, MIP-3α, TNF-α, IL-22 and IL-13 augmented significantly after 12 h treatment of LPS. Co-administration with GYY4137 alleviated the increase of IFN-γ, but made no differences on the other 7 kinds of increased cytokines (Fig. 3G). After 7 days of colitis induced by LPS, although the overall cytokine levels were much lower than that of 12 h, 9 kinds of cytokines (IL-17F, IL-22, IL-17, IL-23, IFN-γ, TNF-α, IL-13, IL-5 and IL-10) in plasma were still elevated in mice of LPS group compared with control group, and GYY4137 attenuated the increase of 6 of them, including IL-17F, IL-22, IL-17, IL-23, IFN-γ and TNF-α (Fig. 3H). These results indicated that $CBS^{-/+}$ mice were more sensitive to the systemic inflammation responses in LPS induced colitis, and exogenous H_2S significantly ameliorated both the local inflammation and the systemic inflammation responses.

H_2S inhibited the expression of COX-2 in mice colon epithelium

Considering the intricate relationship between the LPS induced inflammatory responses and COX-2, we detected the COX-2 expression of mice colon epithelial cells in each group (Fig. 4A, B and C; SI, Fig.S2B and C). The expression of COX-2 and HuR in colon epithelium increased significantly in mice with experimental colitis induced by LPS compared with control group. Co-administration with GYY4137 prominently inhibited the augmented expression of COX-2 in both WT and $CBS^{-/+}$ mice of LPS group, but made no differences on the increased expression of HuR (Fig. 4A, B and D; SI, Fig.S2B and C). The s-sulfhydrated HuR was detected by biotin switch assay, and the results showed that the s-sulfhydration level of HuR was significantly increased by GYY4137 in both groups of mice (Fig. 4A, B and E; SI, Fig.S2B and C).

H_2S inhibited the expression of COX-2 by s-sulfhydrating HuR at Cys13

The impact of H_2S on the expression of COX-2 was further investigated with both Caco-2 and HT-29 cells. The knockout efficiency of KO-CBS in the two kind of cells was verified using western blot (Fig. 5A; SI, Fig.S2D and E). Decreased endogenous H_2S levels were validated in CBS-KO cells (Fig. 5B). COX-2 expression increased after CBS knockout, without significant difference on HuR expression levels in both Caco-2 or HT-29 cells (Fig. 5C; SI, Fig.S3A and B). In addition, the s-sulfhydrated HuR (HuR-SSH) expression was significantly decreased after knocking out CBS (Fig. 5D; SI, Fig.S3C and D).

For the purpose of validating the impact of s-sulfhydration of HuR on the expression of COX-2, plasmids expressing WT HuR (HuR^{WT}) and mutated HuR with single-site mutation of Cys13 to alanine (HuR^{C13A}) were respectively transfected into Caco-2 cells. The results indicated that the overexpression of either HuR^{WT} or HuR^{C13A} increased the expression of COX-2 in Caco-2 cells (Fig. 5E; SI, Fig.S3E). However, GYY4137 failed to inhibit the expression of COX-2 in cells transfected with HuR^{C13A}, and GYY4137 also failed to s-sulfhydrate the HuR expressed in cells transfected with HuR^{C13A} (Fig. 5E; SI, Fig.S3E). ActD chase assay was further performed in Caco-2 cells to investigate the stability of HuR mRNAs. The results showed that in cells treated with ActD alone, the half-life of COX-2 mRNA was about 3.6 h. While in cells administered with ActD + GYY4137, the half-life of COX-2 mRNA was about 1.2 h (Fig. 5F). These results indicated that the s-sulfhydration of HuR mediated by H_2S might be the mechanism underlying the protective effect of CBS-H_2S axis on both local and systemic inflammation responses accompanying the experimental colitis.

Discussion

As the first line to defense against the luminal content, the intestinal barrier system is a prerequisite for the homeostasis of the intestinal ecosystem. Intestinal barrier injuries play an important role in the initiation and propagation of multiple diseases, including inflammatory bowel diseases, necrotizing enterocolitis and so on. During colitis, the increased intestinal permeability, aka "leaky gut", allows tremendous flux of noxious contents and antigens into the intern milieu, which further aggravates the destruction of the intestinal barrier and boosts both local and systemic inflammation responses [23]. Seeking protective reagents against the intestinal barrier function might provide promising therapeutic approaches for colitis.

H_2S plays a vital role in the pathogenesis of various diseases including cancer and inflammatory diseases [24,25]. The inhibiting effect of exogenous H_2S on the intestinal inflammation has been validated [26,27]. Our previous studies found that the expression of CBS declined at the lesion sites of UC, and indicated that CBS knockdown exaggerated the barrier injuries caused by TNF-α/IFN-γ in Caco-2 monolayers [28]. However, the role of CBS-H_2S axis on the development of experimental colitis in vivo and the underlying mechanism remains to be explored.

In this study, experimental colitis was induced by LPS in WT and $CBS^{-/+}$ mice. The results indicated that, after the intraperitoneal injection of LPS, the body weight and clinical scores of

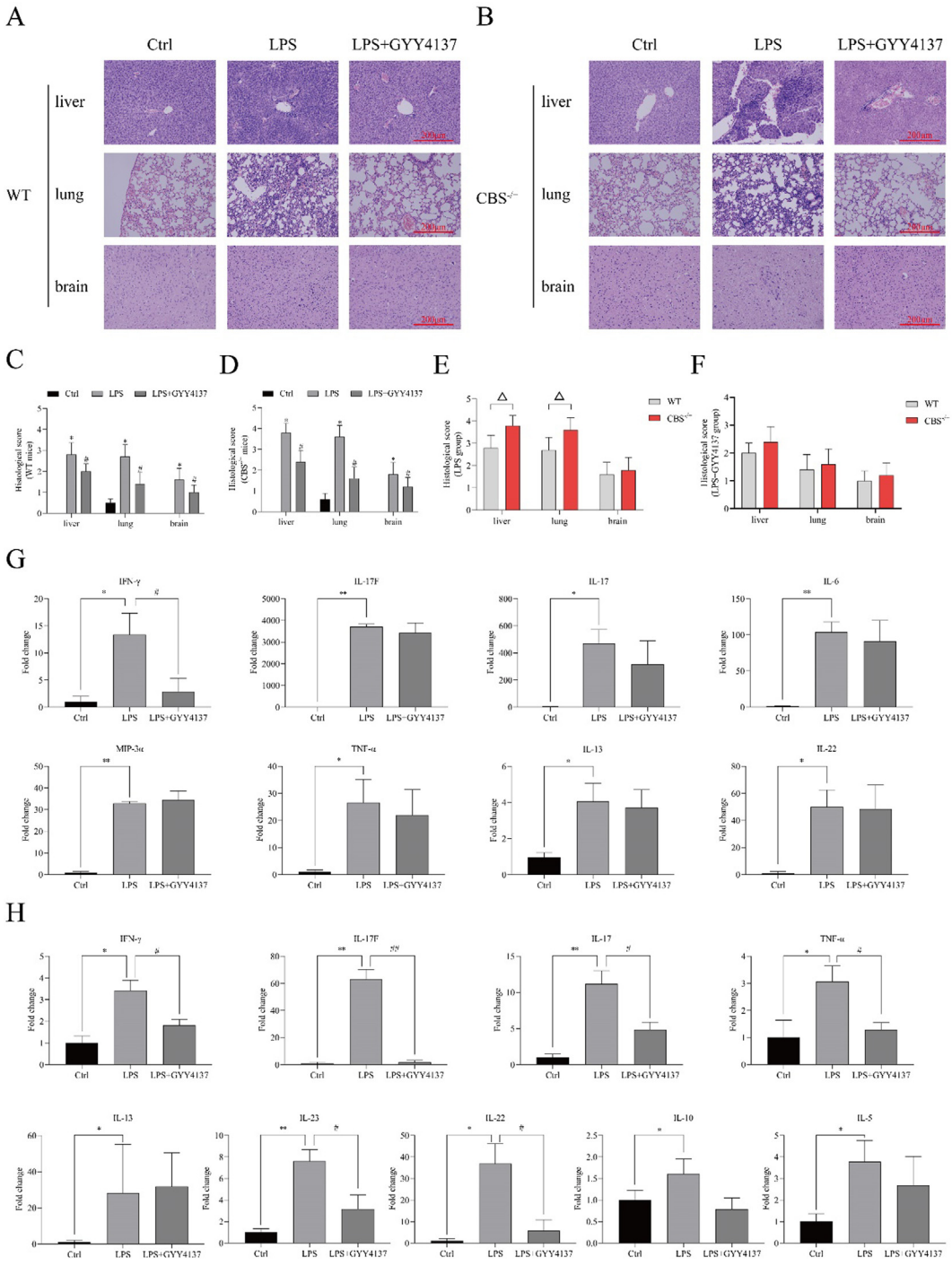

Fig. 3. H_2S attenuated the inflammatory responses of multiple-organs and the increased level of inflammatory cytokines in systemic circulation. **(A, B)** Representative images of HE staining of liver, lung and brain tissue of WT and $CBS^{-/+}$ mice 7 days after LPS administration with or without GYY4137. **(C, D)** Histological score of liver, lung and brain tissue of WT and $CBS^{-/+}$ mice. **(E)** Comparison of histological scores of livers, lungs and brains between WT and $CBS^{-/+}$ mice from LPS group at the 7th day. **(F)** Comparison of histological scores of livers, lungs and brains between WT and $CBS^{-/+}$ mice from LPS + GYY4137 group at the 7th day. **(G)** Quantitative measurement of 18 mouse TH1/TH2/TH17 cytokines in WT mice plasma 12 h after LPS administration with or without GYY4137. **(H)** Quantitative measurement of 18 mouse TH1/TH2/TH17 cytokines in WT mice plasma 7 days after LPS administration with or without GYY4137.

$CBS^{-/+}$ mice decreased more quickly compared with WT mice, and the recoveries of clinical scores was slower. A more remarkable increase of intestinal permeability was also noticed. Electron microscope analysis indicated that after intraperitoneal injection of LPS, the microvilli on the surface of the mouse colonic epithelium were destroyed, the tight junctions between epithelial cells became larger, and the mitochondria in the epithelial cells swelled. Also, CBS knockdown aggravated these pathological ultrastructure alterations in mouse colon epithelium. Histological assessment of colon, liver, lung and brain indicated that the degree of inflammation in these tissues increased after CBS knockdown. For both WT and $CBS^{-/+}$ mice, administration of exogenous H_2S donor GYY4137 attenuated the injuries of intestinal barrier function and distant organs. The levels of 18 kinds of inflammatory cytokines in the plasma of mice with colitis were measured and the results indicated that at 12 h after inducing colitis, the levels of 7

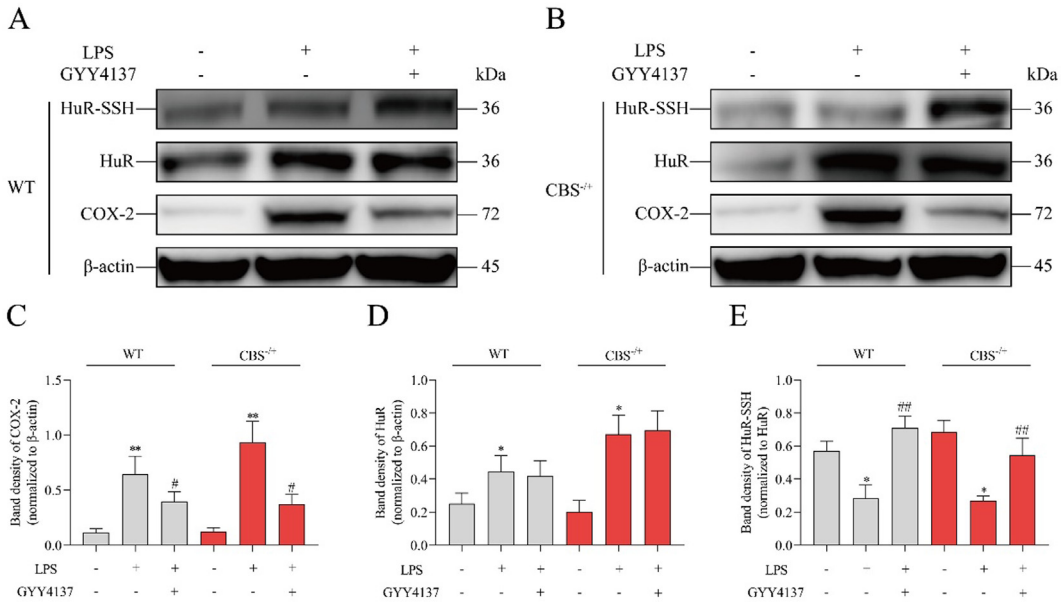

Fig. 4. H_2S attenuated the the increased expression of COX-2 in colon epithelium induced by LPS. **(A)** Representative western blot images of β-actin, COX-2, HuR and HuR-SSH in colon epithelium cells of WT mice. **(B)** Representative western blot images of β-actin, COX-2, HuR and HuR-SSH in colon epithelium cells of $CBS^{-/+}$ mice. **(C, D, E)** Relative band intensity.

kinds of the cytokines in plasma increased significantly, and the administration of GYY4137 attenuated the increase of IFN-γ. At the 7th day after administration of LPS, the levels of 9 cytokines in plasma were still elevated, while the increase of 6 cytokines among them were attenuated by the administration of GYY4137. These results indicated that the decreased CBS-H_2S axis aggravated the intestinal barrier dysfunction and injuries related with systemic inflammation in the mice model of experimental colitis. Based on these results, we set out to research on the mechanism underlying the anti-inflammation effect of H_2S on experimental colitis.

As one of the three known isoforms of cyclooxygenase, COX-2 signaling has been validated to play a pivotal role in impairing intestinal epithelial regeneration and propagating inflammation responses in colitis [29]. Increased expression of COX-2 prompted the release of proinflammatory cytokines from monocytes in flaring colitis [30–32]. The expression level of COX-2 and its mRNA is relatively low under normal circumstances, and the COX-2 mRNA is usually rapidly degraded in normal colon epithelium [33]. However, COX-2 expression could be significantly upregulated by multiple inflammation related stimuli including bacterial derived LPS, inflammation cytokines and various stresses [34]. Recent studies have shown that the level of COX-2 mRNA also depended on its degradation rate, which was under the regulation of RNA binding proteins [11,12]. As an RNA binding protein targeting ARE areas in the 3′-UTR of mRNAs, HuR is mainly located in nucleus. However, inflammation elicited increased shuttling of HuR from the nucleus to the cytoplasm, and improved the regulatory effect of HuR on target mRNAs [35,36]. Previous studies have shown that HuR could stabilize COX-2 mRNA in human mesangial cells, myeloid leukocytes, human duct smooth muscle cells and vascular smooth muscle cells [37–40]. What's intriguing was that recent studies have validated the inhibitory effect of s-sulfhydration mediated by H_2S on the proper function of HuR homodimers [10].

Based on these results and previous reports, we hypothesized that the CBS-H_2S axis could inhibit the expression of COX-2 through s-sulfhydrating HuR and thus inhibiting the formation of homodimers of HuR. Our results indicated that in LPS induced colitis, the expression of COX-2 and HuR in the intestinal epithelial tissues of both WT and $CBS^{-/+}$ mice increased significantly, while administration of GYY4137 decreased the expression of COX-2 without significant changes of the expression of HuR. We detected the s-sulfhydration of HuR by a biotin switch assays and western blot and found that when GYY4137 was administered, the s-sulfhydration of HuR was significantly increased. CRISPR/Cas9 was adopted to knock out CBS in Caco-2 and HT-29 cells, and the results indicated that CBS knockout significantly decreased the s-sulfhydration levels of HuR and augmented the expression of COX-2. Previous studies have reported that HuR could be s-sulfhydrated at the13th cysteine. In the present study, plasmids expressing wild type HuR (HuR^{WT}) and HuR with cysteine 13 mutated to alanine (HuR^{C13A}) were respectively transferred into Caco-2 cells. The results illustrated that the expression of COX-2 was significantly increased after HuR overexpression. GYY4137 increased the s-sulfhydration level of HuR and decreased the expression of COX-2 in cells transfected with HuR^{WT}. However, in cells transfected with HuR^{C13A}, the expression of COX-2 remained unchanged after the administration of GYY4137. Furthermore, we detected the stability of COX-2 mRNA in cells through ActD chase assay and found that GYY4137 significantly declined the stability of COX-2 mRNA in Caco-2 cells. These results indicated that CBS-H_2S axis reduced the stability of COX-2 mRNA and the expression level of COX-2 by increasing the s-sulfhydration level of HuR at cysteine13, which could be one of the potential mechanisms of the anti-inflammation effect of CBS-H_2S axis both locally and systematically. HuR contains three cysteines, and the cysteine at amino acid 13 (Cys13) is highly nucleophilic and can be sulfhydrated by endogenous hydrogen sulfide. It has been reported that Cys13 is important for the formation of HuR dimer, which has stable activity, and the sulfhydration of Cys13 leads to the formation of HuR monomer, which is inactive to bind to the target mRNAs [10]. Increased H_2S may render a higher proportion of HuR in monomer form through sulfhydrating Cys13 in HuR, which inhibit the function of HuR in stabilizing COX-2 mRNA, thus causing the degradation of COX-2 mRNA and reducing the expression of COX-2.

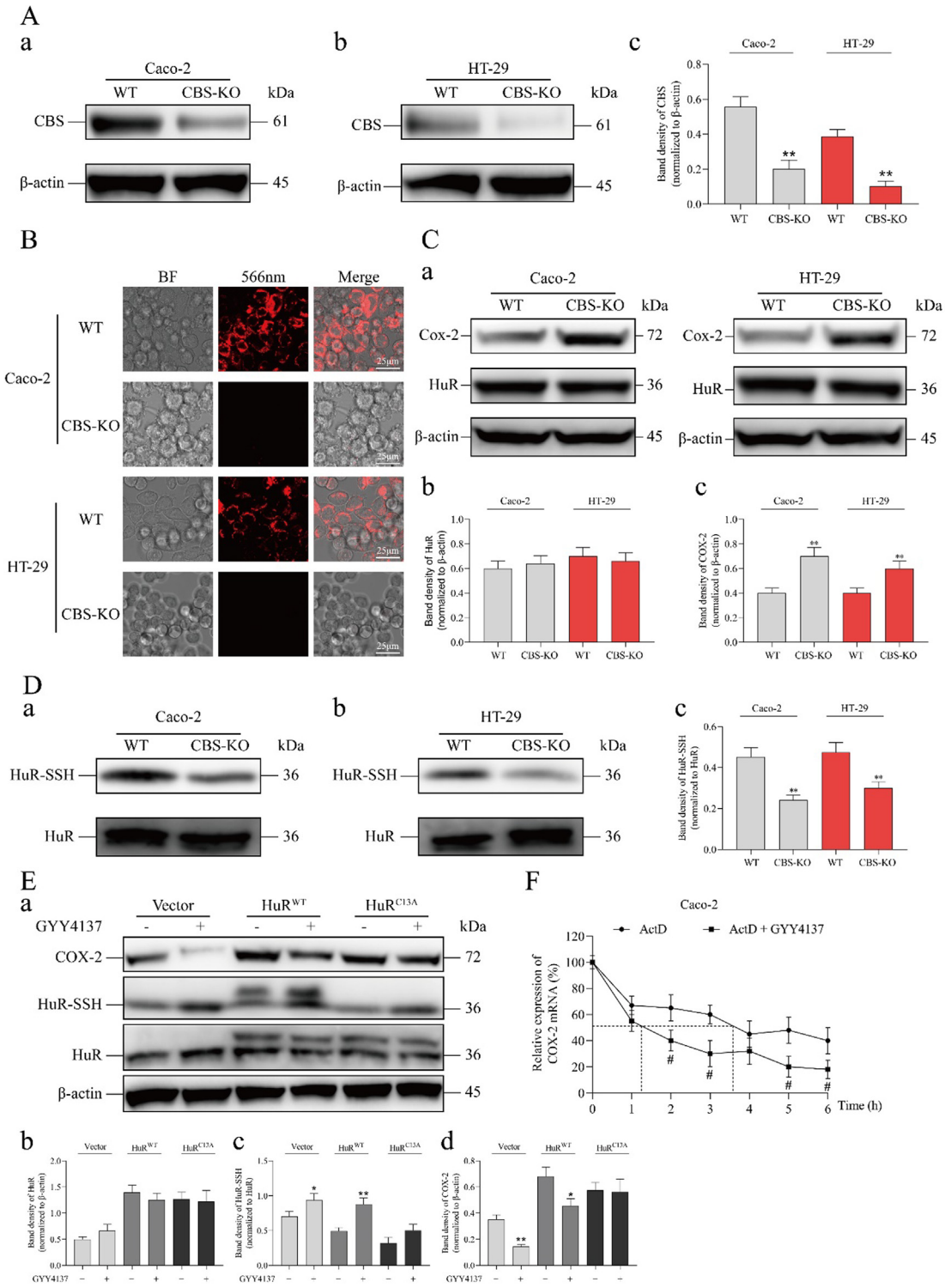

Fig. 5. CBS-H_2S axis decreased the stability of COX-2 mRNA as well as the expression level of COX-2 by s-sulfhydrating HuR. **(A)** Western blot analysis of CBS in different cells. **(a)** Representative western blot images of Caco-2 cells. **(b)** Representative western blot images of HT-29 cells. **(c)**Relative band intensity. **(B)** H_2S level in different cells, measured by H_2S probe. **(C)** Western blot analysis of HuR and COX-2 in different cells. **(a)** Representative western blot images of Caco-2 and HT-29 cells. **(b, c)** Relative band intensity. **(D)** Western blot analysis of HuR and HuR-SSH in different cells. **(a)** Representative western blot images of Caco-2 cells. **(b)** Representative western blot images of HT-29 cells. **(c)** Relative band intensity. **(E)** Western blot analysis of HuR, HuR-SSH and COX-2 in Caco-2 cells after transfected HuR plasmid and the relative band intensity. **(a)** Representative western blot images. **(b-d)** Relative band intensity. **(F)** ActD chase assays for the stability of COX-2 mRNA in Caco-2 cells treated with or without GYY4137. * P < 0.05, ** P < 0.01, vs WT group. # P < 0.05, ## P < 0.01, vs ActD group.

In this study, some novel methods were applied in vitro and in vivo. We established a CBS knockdown mouse strain to verify the protective effect of CBS-H_2S axis in mice with colitis. When detecting the content of H_2S in cells, we used a new type of H_2S probe, which is more intuitive and sensitive than the traditional lead acetate method [22]. Also, a mutated HuR protein, in which cysteine at amino acid site 13 mutated into alanine, was synthesized, by which the sulfhydrated site of HuR was confirmed.

In conclusion, our study showed for the first time that the CBS-H_2S axis played a vital role in protecting the intestinal barrier function in sepsis, and suggested that the inhibition of the stability of COX-2 mRNA by increasing the s-sulfhydration of HuR could be one of the mechanisms underlying the anti-inflammation effect of the CBS-H_2S axis on colitis and potentially other disorders.

Compliance with Ethics Requirements

All Institutional and National Guidelines for the care and use of animals (fisheries) were followed.

Credit author statement

Shihao Guo is in charge of investigation and methodology. Zhihao Huang and Jing Zhu are in charge of the validation and visualization. Taohua Yue is in charge of data duration. Xin Wang and Yisheng Pan contributed to project administration and software. Yucun Liu is in charge of funding acquisition. Pengyuan Wang is in charge of supervision and writing-review & edit. Shanwen Chen is in charge of writing-original draft and formal analysis. All the authors have read and approved the final manuscript.

Declaration of Competing Interest

The authors declare that they have no known competing financial interests or personal relationships that could have appeared to influence the work reported in this paper.

Acknowledgment

The authors wish to acknowledge Dr. Ruijun Wu from the School of Pharmaceutical Sciences of Peking University for her excellent technical assistance.

Funding

This work was supported by grants from the National Natural Science Foundation of China (No. 81902384, No. 81770522), Scientific Research Seed Fund of Peking University First Hospital (No. 2019SF01) and National Science and Technology Major Project of China (2018ZX10723204).

Appendix A. Supplementary material

Supplementary data to this article can be found online at https://doi.org/10.1016/j.jare.2022.03.010.

References

[1] Camilleri M. Leaky gut: mechanisms, measurement and clinical implications in humans. Gut 2019;68(8):1516–26. doi: https://doi.org/10.1136/gutjnl-2019-318427.
[2] Keane TJ, Dziki J, Sobieski E, Smoulder A, Castleton A, Turner N, et al. Restoring Mucosal Barrier Function and Modifying Macrophage Phenotype with an Extracellular Matrix Hydrogel: Potential Therapy for Ulcerative Colitis. J Crohns Colitis 2017 Mar 1;11(3):360–8. doi: https://doi.org/10.1093/ecco-jcc/jjw149.
[3] Chang J, Leong RW, Wasinger VC, Ip M, Yang M, Phan TG. Impaired intestinal permeability contributes to ongoing bowel symptoms in patients with inflammatory bowel disease and mucosal healing. Gastroenterology 2017;153(3):723–731.e1. doi: https://doi.org/10.1053/j.gastro.2017.05.056.
[4] Dilek N, Papapetropoulos A, Toliver-Kinsky T, Szabo C. Hydrogen sulfide: An endogenous regulator of the immune system. Pharmacol Res 2020;161:105119. doi: https://doi.org/10.1016/j.phrs.2020.105119.
[5] Chen S, Zuo S, Zhu J, Yue T, Bu D, Wang X, et al. Decreased Expression of Cystathionine β-Synthase Exacerbates Intestinal Barrier Injury in Ulcerative Colitis. J Crohns Colitis 2019;13(8):1067–80. doi: https://doi.org/10.1093/ecco-jcc/jjz027.
[6] Jensen AR, Drucker NA, Olson KR, Markel TA. Stem Cell Therapy and Hydrogen Sulfide: Conventional or Nonconventional Mechanisms of Action? Shock 2020 Jun;53(6):737–43. doi: https://doi.org/10.1097/SHK.0000000000001420.
[7] Te Winkel J, John QE, Hosfield BD, Drucker NA, Das A, Olson KR, et al. Mesenchymal stem cells promote mesenteric vasodilation through hydrogen sulfide and endothelial nitric oxide. Am J Physiol Gastrointest Liver Physiol 2019 Oct 1;317(4):G441–6. doi: https://doi.org/10.1152/ajpgi.00132.2019.
[8] Kafasla P, Skliris A, Kontoyiannis DL. Post-transcriptional coordination of immunological responses by RNA-binding proteins. Nat Immunol 2014 Jun;15(6):492–502. doi: https://doi.org/10.1038/ni.2884.
[9] Khabar KS. Post-transcriptional control during chronic inflammation and cancer: a focus on AU-rich elements. Cell Mol Life Sci 2010 Sep;67(17):2937–55. doi: https://doi.org/10.1007/s00018-010-0383-x.
[10] Bibli S-I, Hu J, Sigala F, Wittig I, Heidler J, Zukunft S, et al. Cystathionine γ Lyase Sulfhydrates the RNA Binding Protein Human Antigen R to Preserve Endothelial Cell Function and Delay Atherogenesis. Circulation 2019 Jan 2;139(1):101–14. doi: https://doi.org/10.1161/CIRCULATIONAHA.118.034757.
[11] Dixon DA, Kaplan CD, McIntyre TM, Zimmerman GA, Prescott SM. Post-transcriptional control of cyclooxygenase-2 gene expression. The role of the 3'-untranslated region. J Biol Chem 2000 Apr 21;275(16):11750–7. doi: https://doi.org/10.1074/jbc.275.16.11750.
[12] Dixon DA, Tolley ND, King PH, Nabors LB, McIntyre TM, Zimmerman GA, et al. Altered expression of the mRNA stability factor HuR promotes cyclooxygenase-2 expression in colon cancer cells. J Clin Invest 2001 Dec;108(11):1657–65. doi: https://doi.org/10.1172/JCI12973.
[13] Kadl A, Pontiller J, Exner M, Leitinger N. Single bolus injection of bilirubin improves the clinical outcome in a mouse model of endotoxemia. Shock 2007 Nov;28(5):582–8. doi: https://doi.org/10.1097/shk.0b013e31804d41dd.
[14] Brayden DJ, Maher S, Bahar B, Walsh E. Sodium caprate-induced increases in intestinal permeability and epithelial damage are prevented by misoprostol. Eur J Pharm Biopharm 2015 Aug;94:194–206. doi: https://doi.org/10.1016/j.ejpb.2015.05.013.
[15] Chiu CJ, McArdle AH, Brown R, Scott HJ, Gurd FN. Intestinal mucosal lesion in low-flow states. I. A morphological, hemodynamic, and metabolic reappraisal. Arch Surg 1970 Oct;101(4):478–83. doi: https://doi.org/10.1001/archsurg.1970.01340280030009.
[16] Wang Y, Wang Q, Wang B, Gu Y, Yu H, Yang W, et al. Inhibition of EZH2 ameliorates bacteria-induced liver injury by repressing RUNX1 in dendritic cells. Cell Death Dis 2020 Dec 1;11(11):1024. doi: https://doi.org/10.1038/s41419-020-03219-w.
[17] Mikawa K, Nishina K, Takao Y, Obara H. ONO-1714, a nitric oxide synthase inhibitor, attenuates endotoxin-induced acute lung injury in rabbits. Anesth Analg 2003 Dec;97(6):1751–5. doi: https://doi.org/10.1213/01.ANE.0000086896.90343.13.
[18] Dagleish MP, Finlayson J, Bayne C, MacDonald S, Sales J, Hodgson JC. Characterization and time course of pulmonary lesions in calves after intratracheal infection with Pasteurella multocida A:3. J Comp Pathol 2010 Feb-Apr;142(2–3):157–69. doi: https://doi.org/10.1016/j.jcpa.2009.10.015.
[19] Ye D, Guo S, Al-Sadi R, Ma TY. MicroRNA regulation of intestinal epithelial tight junction permeability. Gastroenterology 2011 Oct;141(4):1323–33. doi: https://doi.org/10.1053/j.gastro.2011.07.005.
[20] Moriez R, Salvador-Cartier C, Theodorou V, Fioramonti J, Eutamene H, Bueno L. Myosin light chain kinase is involved in lipopolysaccharide-induced disruption of colonic epithelial barrier and bacterial translocation in rats. Am J Pathol 2005 Oct;167(4):1071–9. doi: https://doi.org/10.1016/S0002-9440(10)61196-0.
[21] Lin Z, Altaf N, Li C, Chen M, Pan L, Wang D, et al. Hydrogen sulfide attenuates oxidative stress-induced NLRP3 inflammasome activation via S-sulfhydrating c-Jun at Cys269 in macrophages. Biochim Biophys Acta Mol Basis Dis. 2018 Sep;1864(9 Pt B):2890-2900. doi: 10.1016/j.bbadis.2018.05.023.
[22] Zhang K, Zhang J, Xi Z, Li L-Y, Gu X, Zhang Q-Z, et al. A new H2S-specific near-infrared fluorescence-enhanced probe that can visualize the H2S level in colorectal cancer cells in mice. Chem Sci 2017 Apr 1;8(4):2776–81. doi: https://doi.org/10.1039/c6sc05646f.
[23] Oshima T, Miwa H. Gastrointestinal mucosal barrier function and diseases. J Gastroenterol 2016 Aug;51(8):768–78. doi: https://doi.org/10.1007/s00535-016-1207-z.
[24] Lo Faro ML, Fox B, Whatmore JL, Winyard PG, Whiteman M. Hydrogen sulfide and nitric oxide interactions in inflammation. Nitric Oxide 2014 Sep 15;41:38–47. doi: https://doi.org/10.1016/j.niox.2014.05.014.
[25] Zhu H, Blake S, Chan KT, Pearson RB, Kang J. Cystathionine β-Synthase in Physiology and Cancer. Biomed Res Int 2018 Jun 28;2018:3205125. doi: https://doi.org/10.1155/2018/3205125.
[26] Collin M, Anuar FB, Murch O, Bhatia M, Moore PK, Thiemermann C. Inhibition of endogenous hydrogen sulfide formation reduces the organ injury caused by endotoxemia. Br J Pharmacol 2005 Oct;146(4):498–505. doi: https://doi.org/10.1038/sj.bjp.0706367.
[27] Guo FF, Yu TC, Hong J, Fang JY. Emerging Roles of Hydrogen Sulfide in Inflammatory and Neoplastic Colonic Diseases. Front Physiol 2016 May 3;7:156. doi: https://doi.org/10.3389/fphys.2016.00156.
[28] Chen S-W, Zhu J, Zuo S, Zhang J-L, Chen Z-y, Chen G-W, et al. Protective effect of hydrogen sulfide on TNF-α and IFN-γ-induced injury of intestinal epithelial barrier function in Caco-2 monolayers. Inflamm Res 2015 Oct;64(10):789–97. doi: https://doi.org/10.1007/s00011-015-0862-5.
[29] Li Y, Soendergaard C, Bergenheim FH, Aronoff DM, Milne G, Riis LB, et al. COX-2-PGE2 Signaling Impairs Intestinal Epithelial Regeneration and Associates

with TNF Inhibitor Responsiveness in Ulcerative Colitis. EBioMedicine 2018 Oct;36:497–507. doi: https://doi.org/10.1016/j.ebiom.2018.08.040.
[30] Tanabe T, Tohnai N. Cyclooxygenase isozymes and their gene structures and expression. Prostaglandins Other Lipid Mediat 2002 Aug;68-69:95–114. doi: https://doi.org/10.1016/s0090-6980(02)00024-2.
[31] Sato N, Kozar RA, Zou L, Weatherall JM, Attuwaybi B, Moore-Olufemi SD, et al. Peroxisome proliferator-activated receptor gamma mediates protection against cyclooxygenase-2-induced gut dysfunction in a rodent model of mesenteric ischemia/reperfusion. Shock 2005 Nov;24(5):462–9. doi: https://doi.org/10.1097/01.shk.0000183483.76972.ae.
[32] Zamuner SR, Warrier N, Buret AG, MacNaughton WK, Wallace JL. Cyclooxygenase 2 mediates post-inflammatory colonic secretory and barrier dysfunction. Gut 2003 Dec;52(12):1714–20. doi: https://doi.org/10.1136/gut.52.12.1714.
[33] Sully G, Dean JL, Wait R, Rawlinson L, Santalucia T, Saklatvala J, et al. Structural and functional dissection of a conserved destabilizing element of cyclooxygenase-2 mRNA: evidence against the involvement of AUF-1 (AU-rich element/poly(U)-binding/degradation factor-1), AUF-2, tristetraprolin, HuR (Human antigen R) or FBP1 (far-upstream-sequence-element-binding protein 1). Biochem J 2004 Feb 1;377(Pt 3):629–39. doi: https://doi.org/10.1042/BJ20031484.
[34] Kim MH, Kang SG, Park JH, Yanagisawa M, Kim CH. Short-chain fatty acids activate GPR41 and GPR43 on intestinal epithelial cells to promote inflammatory responses in mice. Gastroenterology 2013 Aug;145(2):396–406–410. doi: https://doi.org/10.1053/j.gastro.2013.04.056.
[35] Cok SJ, Morrison AR. The 3'-untranslated region of murine cyclooxygenase-2 contains multiple regulatory elements that alter message stability and translational efficiency. J Biol Chem 2001 Jun 22;276(25):23179–85. doi: https://doi.org/10.1074/jbc.M008461200.
[36] Abdelmohsen K, Gorospe M. Posttranscriptional regulation of cancer traits by HuR. Wiley Interdiscip Rev RNA 2010 Sep-Oct;1(2):214–29. doi: https://doi.org/10.1002/wrna.4.
[37] Young LE, Moore AE, Sokol L, Meisner-Kober N, Dixon DA. The mRNA stability factor HuR inhibits microRNA-16 targeting of COX-2. Mol Cancer Res 2012 Jan;10(1):167–80. doi: https://doi.org/10.1158/1541-7786.MCR-11-0337.
[38] Doller A, Akool El-S, Huwiler A, Müller R, Radeke HH, Pfeilschifter J, et al. Posttranslational modification of the AU-rich element binding protein HuR by protein kinase Cdelta elicits angiotensin II-induced stabilization and nuclear export of cyclooxygenase 2 mRNA. Mol Cell Biol 2008 Apr;28(8):2608–25. doi: https://doi.org/10.1128/MCB.01530-07.
[39] Lin WN, Lin CC, Cheng HY, Yang CM. Regulation of cyclooxygenase-2 and cytosolic phospholipase A2 gene expression by lipopolysaccharide through the RNA-binding protein HuR: involvement of NADPH oxidase, reactive oxygen species and mitogen-activated protein kinases. Br J Pharmacol 2011 Aug;163(8):1691–706. doi: https://doi.org/10.1111/j.1476-5381.2011.01312.x.
[40] Aguado A, Rodríguez C, Martínez-Revelles S, Avendaño MS, Zhenyukh O, Orriols M, et al. HuR mediates the synergistic effects of angiotensin II and IL-1β on vascular COX-2 expression and cell migration. Br J Pharmacol 2015 Jun;172(12):3028–42. doi: https://doi.org/10.1111/bph.13103.